



## Electrochemical modified electrode with bismuth film for ultrasensitive determination of aluminum (iii)



Maria Camila Ayala<sup>a,b</sup>, Lizbeth Lorena López<sup>c</sup>, Andres Jaramillo-Botero<sup>d,a</sup>, Drochss Valencia<sup>a,\*</sup>

<sup>a</sup> Omicas Program, Pontificia Universidad Javeriana sede Cali, Calle 18 No. 118-250, Cali C.P. 760031, Colombia

<sup>b</sup> Universidad Santiago de Cali, Calle 5 # 62-00 Barrio Pampalinda, Cali, Colombia

<sup>c</sup> Facultad de Ciencias Naturales y Exactas, Universidad del Valle, Cali 760032, Colombia

<sup>d</sup> Chemistry and Chemical Engineering Division, California Institute of Technology, Pasadena, CA 91125, USA

### ARTICLE INFO

#### Keywords:

Bismuth modified electrode  
Electrochemical sensor  
Aluminum detection  
Double potential step chronoamperometry  
Square wave voltammetry

### ABSTRACT

The quantification of heavy metals is crucial to many different applications, and particularly relevant to agriculture. Here we describe an electrochemical sensor to detect and quantify ultra-low concentrations of aluminum in solutions. High aluminum levels are associated with inadequate crop development, growth, and production. To this end, we demonstrate and validate a cheaper glassy carbon electrode modified by the electrochemical reduction of bismuth in an acetate buffer, for square wave voltammetry (SWV) of  $\text{Al}^{3+}$  in a cupferron solution  $0.22 \text{ mmol L}^{-1}$  + ammonium sulfate buffer  $0.4 \text{ mmol L}^{-1}$  pH 5.50, using double-potential pulse chronoamperometry. The proposed method ensures reproducible and stable surface modification of the electrode, and a sensor with linear response in the concentration range of  $1.85 \times 10^{-10}$  to  $3.70 \times 10^{-6} \text{ mol L}^{-1}$  with a detection limit of 0.025 ppb and resistance to interfering metals such as lead (Pb) cadmium (Cd) and zinc (Zn). This type of technology is amenable to industrial scaling and production and could be used for soil characterization and remediation in agriculture, as well as other applications related to food production and safety where accurate and rapid, yet cost-effective, on-site monitoring is required.

### 1. Introduction

Chemically modified electrodes (CME) have become a cornerstone of science and technology due to their wide range of applications, including: electroanalysis [1–15], pathogen biosensors [1,3,16–18], solar energy conversion [3,5,19,20], and others [6–8]. Electrode surfaces can be modified for various purposes and applications. For example, for selective and accurate detection of analytes in various matrices, even at trace levels. The high sensitivity of CME is related to two important variables: the electrochemical technique used to determine the analyte of interest [2,4,7–9,11,14,15,21], and the functionalization or molecular modification on the surface of the electrode [4,6–11,18,21,22].

The best known electrochemical techniques for the determination of analytes in trace amounts are differential pulse voltammetry (DPV) [2,7,8,10,13,21,23] and square wave voltammetry (SWD) [4,7–9,11,12,24]. These techniques consist of at least two steps: (i) preconcentration of the analyte of interest on the surface of the working electrode and (ii) voltammetric determination of the species of interest. Regarding molecular functionality, the sensitivity and speci-

ficity of CME are related to the chemical species modifying the electrode surfaces [2,7–12,22–25].

Carbon materials are widely used as surface materials for the preparation of CMEs due to their diverse physicochemical properties, affordable price, ease of handling, and chemical derivatization [6–10,22,25,26]. Carbon-based CMEs have been used to identify drugs in complex matrices, e.g., urine<sup>6</sup>, to monitor blood glucose levels<sup>6</sup>, for trace levels of heavy metals [2,10,14,27–30] and pollutants in water and soils [4,7–9,22] and more recently for pathogens such as SARS-CoV-2 in saliva or nasopharyngeal fluid [31].

Surface modification of CMEs is conventionally achieved via chemical derivatization [7–9,25,30], electrodeposition [7,8,26], physisorption [2,8,9,13,18,22,27,32,33], chemisorption [7,8,10,14,21], or sputtering [8,34,35]. The type of species used to modify the CME goes hand in hand with the analyte to be determined. For example, heavy metals such as cadmium, chromium, tin and lead can be determined with glassy carbon electrodes modified with deposits of metal-organic frameworks (MOFs) [4], electrolytic deposits of conductive polymers [7], zeolites [27–30,33] and bismuth films [8,21,22]. CMEs have also been used on other heavy metals, such as zinc, cadmium, lead, arsenic,

\* Corresponding author.

E-mail address: [drochss.valencia@javerianacali.edu.co](mailto:drochss.valencia@javerianacali.edu.co) (D. Valencia).

copper, and aluminum for soil, air, and water remediation. High concentrations of lead, chromium and arsenic can seriously affect human health because they accumulate in the body and are difficult to eliminate, negatively affecting organs such as the kidney, liver, brain, and bones [36].

In general, measurement of heavy metal content in different matrices helps characterize environmental systems and conditions. For example, the presence and absence of cadmium, zinc, and copper, and changes in their concentrations, alter several metabolic processes that are closely correlated with degenerative abnormalities in plants [37]. In agriculture, the amount of aluminum has been associated with inadequate crop development, growth, and production. Aluminum ion ( $\text{Al}^{3+}$ ) uptake impairs synthesis, cell expansion, and nutrient transfer from plant roots to main stems, affecting their overall metabolism [38,39]. Consequently, chemical quantification of  $\text{Al}^{3+}$  in plant tissues provides important clues for understanding its effects on plant metabolism. In addition, quantification of  $\text{Al}^{3+}$  in agricultural soils is an indicator of its bioavailability. Various methods for measuring  $\text{Al}^{3+}$  content have been reported in the literature, including spectroscopic [12,40,41], electrochemical [12–14], and others [42,43]. In most cases, sample preparation is tedious but crucial, and measurements require complex protocols and expensive equipment.

Here we report a bismuth-modified electrode for the detection and measurement of aluminum concentration in soils. The proposed method for modifying the electrode surface involves complexation of the metal with a ligand and mass transfer between the surface and a solution. These results contribute to the growing need for rapid, economical, and on-site analysis of various types of metals that are toxic to both the environment and human health, and demonstrate the advantages of electrochemical techniques over alternatives such as chromatography or spectroscopy.

## 2. Materials and methods

### 2.1. Reagents

Aluminum 1000 mg  $\text{L}^{-1}$  (MOL LABS  $\geq 99,0\%$ ), Sodium borohydride (Panreac, 96%), and all other reagents were acquired from Merck, including: bismuth nitrate ( $\text{Bi}(\text{NO}_3)_3$ ), cupferron (97%), PIPES ( $\geq 99\%$ ), ammonia solution (23%), sulfuric acid ( $\geq 99\%$ ), acetic acid ( $\geq 99\%$ ), sodium hydroxide ( $\geq 99\%$ ).

For the electrode polishing process, 0.30 and 1.00  $\mu\text{m}$  alumina (Buehler micropolish) and absolute ethanol ( $\geq 99.8\%$ ) were used. All solutions were prepared with deionized water having a resistivity of 18  $\text{M}\Omega\text{cm}^{-1}$  obtained in a Milli-Q purification system (Millipore).

### 2.2. Instruments

Electrochemical measurements were performed with a Metrohm Autolab potentiostat-galvanostat, model PGSTAT302N, coupled and controlled from an ASUS PC using NOVA 2.1 software. A three-electrode electrochemical cell was used. A 3.0 mol  $\text{L}^{-1}$  Ag/AgCl/KCl electrode and a platinum mesh counter electrode were used as the reference electrode. The working electrode was a 3.00 mm diameter glassy carbon electrode, which was modified according to the procedures described in the following section. All electrochemical experiments were conducted at room temperature (25 °C).

### 2.3. Electrodes cleaning and polishing

Mechanical smoothing of the surface of glassy carbon electrodes involved: 1) Sanding the surface using a water sandpaper, and subsequently, 2) polishing it with a Buehler polisher at 200 rpm using a microfiber cloth with 1.00  $\mu\text{m}$  alumina powder for about 10 min, 3) washing with distilled water, 4) re-polishing with 0.30  $\mu\text{m}$  alumina

for the same amount of time, and 5) sonicating in ethanol for 15 min according to the procedures described in the literature [30].

### 2.4. Production of the bismuth CME

Glassy carbon electrodes were electrochemically modified by applying a double potential pulse in an electrochemical cell containing 10.00 mL of an aqueous solution of  $\text{Bi}(\text{NO}_3)_3$  5.00 mmol  $\text{L}^{-1}$ , in acetic acid/sodium acetate buffer pH 4.50, 1.00 mol  $\text{L}^{-1}$  by Cyclic voltammetric (CV) and Double potential step chronoamperometry (DPSC). The electrochemical reduction of bismuth was carried out starting from an initial potential ( $E_0$ ) of 0.00 V for 60 s until a final potential of  $E_f = -1.00$  V was reached for a period of 300 s. In this procedure, the potential of the working electrode is fixed at a value suitable to initiate the faradaic processes at the electrode surface (caused by the potential jump) in order to monitor the resulting current over time. To perform the chronoamperometric measurements, both single and double potential jumps can be performed on the working electrode, as described in the literature [44].

After the modification, let the system equilibrate for 10 s and rinse the working electrode with distilled water. CV was used to characterize electrode modification in a bismuth-free buffer solution at a pH of 4.50, using oxidation potential sweep from  $-0.35$  V to 0.40 V at a scan rate of 0.100  $\text{V s}^{-1}$ .

### 2.5. Determination of Al (III)

We added  $\text{Al}^{3+}$  to solutions containing 5.00 mL of cupferron 0.22 mmol  $\text{L}^{-1}$  dissolved in ammonium sulfate 0.40 mmol  $\text{L}^{-1}$ , pH = 5.50, and recorded CVs after modifying the bismuth glassy carbon electrode surface, which also modified the electrode between each measurement. The anodic peaks corresponding to  $\text{Al}^{3+}$  showed different behaviors depending on the surface modifications.

## 3. Results and discussion

To determine the best experimental conditions for bismuth electrode (BiE) fabrication and operation, we considered several surface modification variables including: Deposition potential, deposition time, bismuth concentration, pH, electrode surface cleaning, and electrochemical techniques for surface modification. These are discussed in the following subsections.

### 3.1. Electrochemical techniques for surface modification of glassy carbon electrodes

CV and DPSC were used to evaluate which technique works best in the fabrication of BiE. We selected the technique that provided the best film synthesis reproducibility, the shortest modification time, the simplest cleaning, and the simplest electrochemical technique.

#### 3.1.1. Glassy carbon surface modification using CV

For bismuth glassy carbon surface modification by CV, we started with an initial potential of  $-0.30$  V to a final potential of  $-1.50$  V with respect to the reference potential of Ag/AgCl and returned to the initial potential in a solution containing bismuth at 3.00 mmol  $\text{L}^{-1}$ .

The voltammogram shows a slight passivation between cycles, as shown in the inset of Fig. 1A. However, the modification on the glassy carbon surface with the bismuth film was indirectly evaluated by the electrochemical oxidation of the modified surface in the previous step, for which the electrode was washed rinsed with ethanol and water and transferred to an electrochemical cell containing a bismuth-free acetate/acetic acid buffer solution with a pH of 4.50 (blank solution), we observed the cathodic current peak ( $I_a$ ) at  $-0.050$  V using a poten-

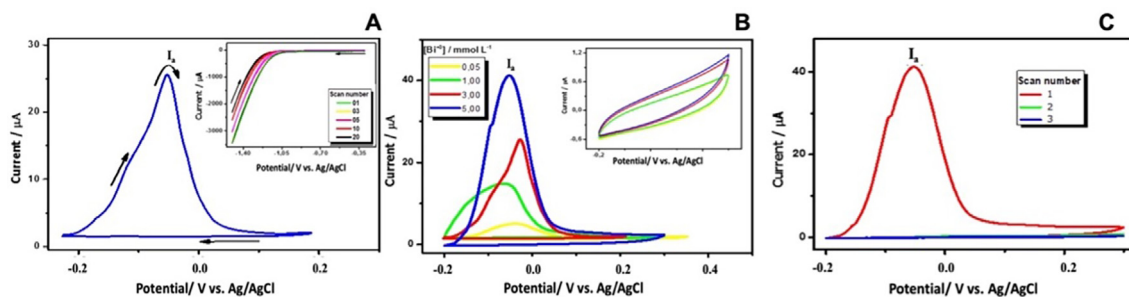


**Fig. 1.** CV response of carbon surfaces modified with a bismuth film by the electrochemical reduction of  $\text{Bi}(\text{NO}_3)_3$   $3.00 \text{ mmol L}^{-1}$  + acetate/acetic acid buffer pH 4.50 scan rate =  $0.100 \text{ V s}^{-1}$  A) Modification of the glassy carbon surface with the bismuth solution, (insert: effect of the scan number on the modification), in the blue line, indirect measurement of the modification of the surface with bismuth by electrochemical oxidation of the electrode surface in a blank solution with free  $\text{Bi}^{3+}$ . B) Effect of the concentration of the bismuth on modification of glassy carbon electrodes by the electrochemical oxidation of the bismuth film in a blank solution C) Removal of the bismuth film by successive electrooxidation of the surface.

tial sweep from  $-0.25 \text{ V}$  to  $0.20 \text{ V}$  vs Ag/AgCl. This current peak is characteristic of the adsorption phenomena exhibited by some surface species [45]. Fig. 1A exhibits a peak current of  $25.50 \mu\text{A}$ , demonstrating the formation of a bismuth film on the carbon electrode, which we refer to as the bismuth electrode (BiE).

When the initial bismuth salt concentration was changed from  $0.0500 \text{ mol L}^{-1}$  to  $5.00 \text{ mmol L}^{-1}$ , the BiE voltamperogram shows changes in the blank solution (Fig. 1B). With increasing bismuth salt concentration, the BiE exhibits a larger current, indicating that additional bismuth is deposited on the carbon surface as expected. The peak current  $I_a$  reached its maximum value when the electrode was modified with a bismuth concentration of  $5.00 \text{ mmol L}^{-1}$ . Experiments were also performed with higher bismuth concentrations, but the low reproducibility of peak current  $I_a$  at these higher concentrations indicated that some of the bismuth film was desorbed and appeared as small particles in the blank solution.

In order to assess the stability of the deposited bismuth film, the electrochemical oxidation of the formed films was investigated via successive potential cycles ranging from  $-0.20 \text{ V}$  to  $0.30 \text{ V}$ , as shown in Fig. 1C. The results show that BiE oxidation completely removes the bismuth film in the first scan cycle. This can be explained based on the species diagram for  $\text{Bi}^{3+}$  ions [46]. When the difference between the potentials exceeds  $0.00 \text{ V}$  vs. NHE, the bismuth is completely oxidized [46].

Fig. 1 clearly shows that bismuth glassy carbon electrode modification is achieved with CV. However, it is not very reproducible, and the stability of the film is also compromised at high concentrations of bis-

moth. We have performed additional studies with successive potential scan to confirm that the BiE can only be used once when oxidized at potentials greater than  $-0.15 \text{ V}$ .

### 3.1.2. Glassy carbon surface modification using DPSC

Glassy carbon electrode was modified by DPSC by immersing it to different concentrations of  $\text{Bi}(\text{NO}_3)_3$  from  $E_0 = 0.00 \text{ V}$  to  $E_f = -1.00 \text{ V}$  during 300 s. The electrode was then washed with copious amounts of water and the degree of modification was evaluated indirectly by CV from  $-0.30 \text{ V}$  to  $0.40 \text{ V}$  in a bismuth free solution of acetic acid/sodium acetate buffer solution at a pH of 4.50. The results of this modification are shown in Fig. 2A and B. We observe that as the concentration of the solution increases, the peak current ( $I_a$ ), also increases indicating that more bismuth has been deposited on the surface of the electrode. If we compare this modification method with the CV method, we see that the peak currents for the modified electrodes are much higher for the same initial conditions. For example, a peak current of  $89.30 \mu\text{A}$  (Fig. 2A) is observed for a  $\text{Bi}^{3+}$   $3.00 \text{ mmol L}^{-1}$  solution by the DPSC modification method, while a current about 3.5 times lower is observed for the CV method when the BiE was formed (Fig. 1A =  $25.50 \mu\text{A}$ ). For this reason, we opted for chronoamperometric method in the production of BiEs.

DPSC allows to control the time and the potential of the deposition, so that we obtain homogeneous and reproducible electrodeposited structures, as it has been shown in the literature for the production of controlled homogeneous surfaces, while continuous cycles by CV

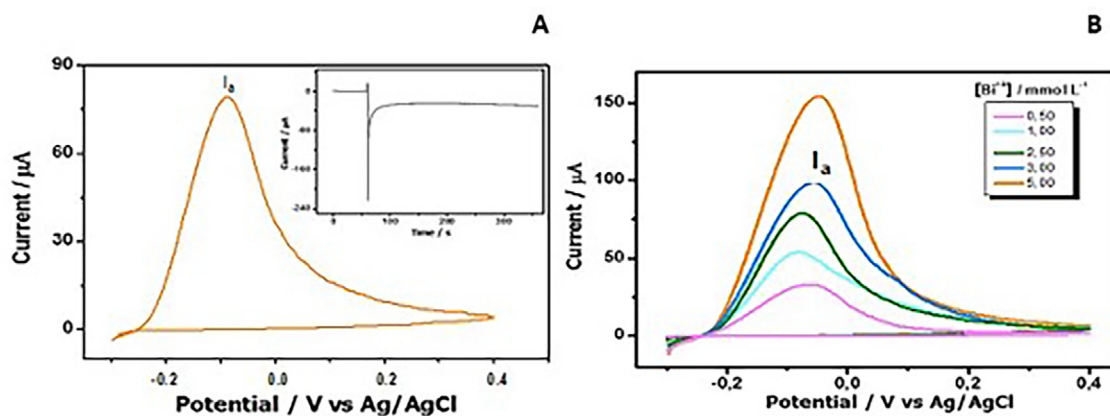


**Fig. 2.** Electrochemically Characterization of glassy carbon surfaces modified with a bismuth film by DPSC from an initial potential of  $0.00 \text{ V}$  to a final potential of  $-1.00 \text{ V}$ , indirectly measured by oxidation of the surface in buffer solution pH 4.5. A) insert Experimental DPSC transients for  $\text{Bi}^{3+}$   $3.00 \text{ mmol L}^{-1}$  solution + acetate/acetic acid buffer pH 4.50 and indirect evaluation of the modification by CV B) Effect of bismuth concentration on modification of glassy carbon electrodes.

produce a constant electro-oxidation/reduction on the surface, making the deposited film inhomogeneous[47–49].

### 3.2. Effect of the final potential applied in the BiE formation

To determine the potential at which bismuth electrodeposition occurs on the surface of the glassy carbon electrode, the potential step for DPSC was changed from an initial potential  $E_0$  (0.00 V versus Ag/AgCl) to a final potential  $E_f$  varying between  $-0.10$  V and  $-1.00$  V while maintaining a deposition time of 300 s in a  $\text{Bi}(\text{NO}_3)_3$  5.00 mmol  $\text{L}^{-1}$  at pH 4.50. The current response as a function of time is shown in Fig. 3A. The larger the potential difference, i.e., the more negative the  $E_f$  values, the larger the average current in the current-time transmission. To better understand this phenomenon, the time range shown in Fig. 3A. is 300 s for each potential step and shows only the current change as a function of potential. In the inset of Fig. 3A, we can also see more clearly the dependence of the average current on the potential.

To determine how much  $\text{Bi}^{3+}$  can be deposited between each potential step, the glassy carbon electrode modified with the bismuth layer is washed with abundant amounts of water and placed in ultrasound. Later, for each modification, a CV was prepared in a bismuth-free solution at a pH of 4.50 (see Fig. 3B). This figure shows that at a potential of  $E_f = -0.10$  and  $-0.20$  V, there are no defined peak on the plotted scale, indicating that the carbon electrode surface is not modified with bismuth in this potential range. When modification occurs at a potential  $E_f$  below  $-0.30$  V, the voltametric behavior in Fig. 3B confirms the occurrence of anodic currents from a potential of  $-0.31$  V to a potential with a maximum current of  $-0.020$  V, corresponding to surface oxidation of the previously deposited bismuth. When the carbon surface is modified with even more negative potential transitions, the peak current  $I_p$  increases from an initial current of 63.71  $\mu\text{A}$  to a current of 157.18  $\mu\text{A}$ . We find that the largest potential for the modification at  $-1.00$  V. To confirm this, scanning electron microscope (SEM) images of laser-induced graphene electrodes (LIG) were taken before and after performing each modification at each potential to verify that bismuth deposition on the electrodes occurs at each  $E_f$  (Support information). We still had the Ia peak at the larger potential jumps, and other peaks began to appear (in consistency with the Pourbaix diagram) [46], albeit these are beyond the scope in this article.

To better observe the effects of the applied terminal potential on the BiE current, Fig. 3C was created from the data in Fig. 3B, graphing the peak current as a function of the  $E_f$  potential applied during chronoamperometry. In this figure, we observe that the maximum current increased whenever the  $E_f$  potential for the modification became increasingly negative; in fact, the maximum current is reached when the  $E_f$  potential is  $-1.00$  V. When the  $E_f$  potential for modification was greater than this value, the current decreases. We believe that this is mainly due to two phenomena: a) the continuous accumulation of

bismuth on the surface, which allows the grain to reach a critical size before the current drops due to mechanical detachment (supported by the fact that visually at potentials more negative than  $-1.00$  V, are observed in solution), and b) the fact that at these potentials other chemical species are formed on the surface of the electrode, where the transfer processes can change, albeit the growth of the modification layer can be explained. The maximum current also reflects the amount of bismuth deposited, i.e., the greater the current at a peak adsorption, the greater the amount of species adsorbed, as can be seen from,

$$i_p = \frac{n^2 F^2}{4RT} \nu A \Gamma^* \quad (1)$$

Where  $\Gamma^*$  is the surface coverage of all the adsorbed species in mol  $\text{cm}^{-2}$ ,  $n$  is the number of electrons per molecule,  $F$  is the Faraday constant (96485.15C  $\text{mol}^{-1}$ ),  $T$  is the absolute temperature,  $A$  is the electrode area in  $\text{cm}^2$ ,  $R$  is the universal ideal gas constant in  $\text{J K}^{-1} \text{mol}^{-1}$ , and  $\nu$  corresponds to the scanning speed in  $\text{V s}^{-1}$ .

### 3.3. Effect of bismuth deposition time on the surface of the glassy carbon electrode

To determine the optimum time for modifying the surface of the glassy carbon electrode, DPSC were performed with a solution of bismuth nitrate 5.00 mmol  $\text{L}^{-1}$  in acetic acid/sodium acetate buffer pH 4.50, using various deposition times in the range of 30–600 s. The deposition time was determined from the peak currents, as explained below. The effects of deposition time were evaluated using the maximum current obtained by CV for an empty solution of acetic acid/sodium acetate buffer, with an oxidation sweep from  $-0.20$  V to 0.30 V after each DPSC. These results are shown below in Fig. 4.

From Fig. 4A, we observe that as the deposition time increased in chronoamperometry, the current of anodic peak  $I_p$  in CV increased (in consistency with the longer the deposition time), and more species can diffuse from solution to the electrode's surface, only to become reduced to metallic bismuth. Fig. 4a illustrates the dependence of peak current on applied time. In fact, this dependence was linear over the entire time range studied and showed a correlation coefficient of  $R^2 = 0.995$ .

The reproducibility of the deposition times was evaluated by repeating the previous experiment at least three times for each time. We find that for deposition times of less than 300 s, the changes in peak current  $I_p$  were less than 5%. For longer times, the changes in peak current were not very reproducible. For this reason, we decided to set 300 s as the optimal time value for BiE generation.

### 3.4. Bismuth concentration effect on electrode surface modification

In order to find the optimum bismuth concentration for the modification of glassy carbon electrodes, potential double-pulse chrono-

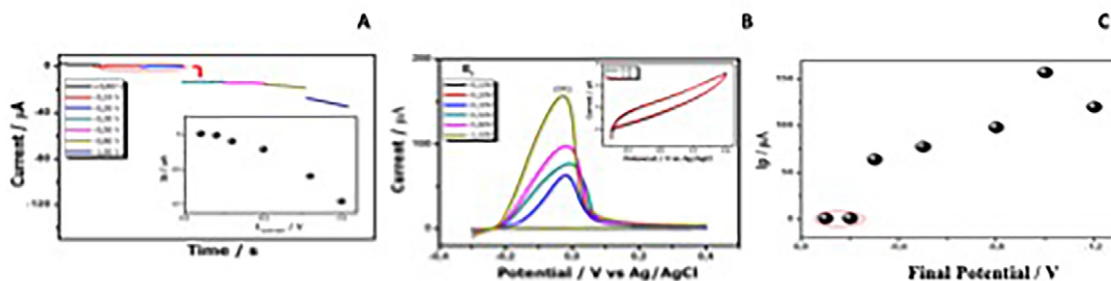


Fig. 3. Dependence of the applied final potential in DPSC curves on the bismuth film thickness from initial potential 0.0 V. time deposition 300 s A) Stepping from 0.0 V to different final potentials at pH 4.50. B) Effect of bismuth concentration on modification of glassy carbon electrodes indirectly measured by oxidation of the electrode surface C) Dependence on peak current with respect to the final potential of Figure B.

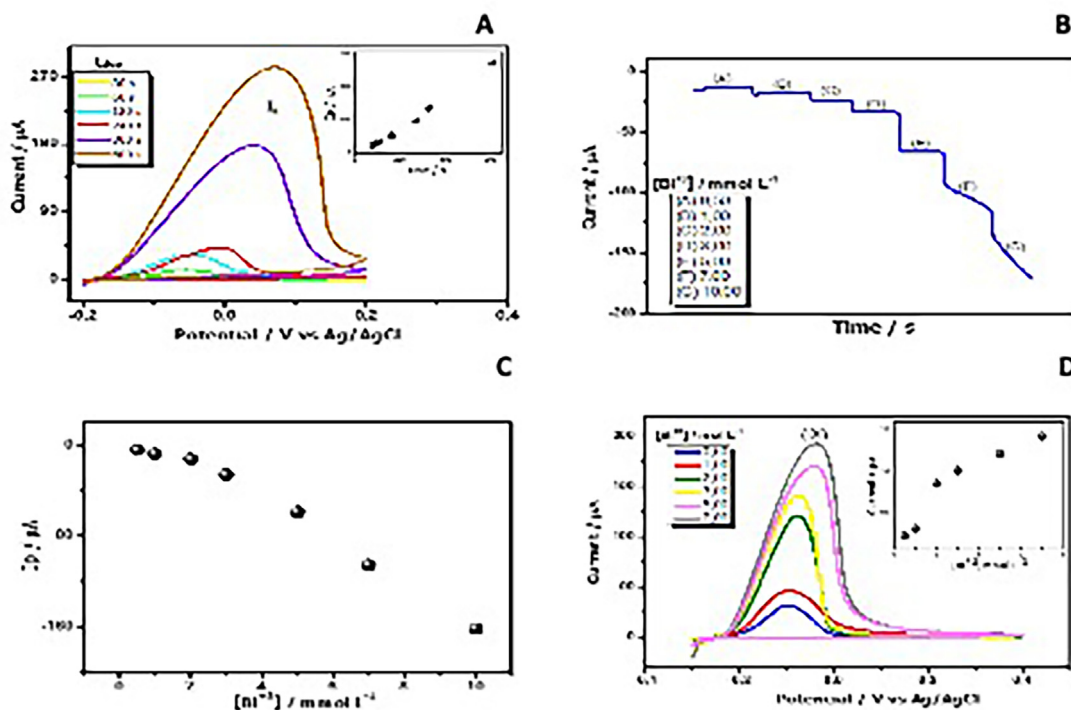


Fig. 4. Dependence of time deposition on bismuth layer thickness for DPSC from initial potential 0.0 V to  $-1.00$  V A) CV curves of BiEs electrodes obtained with different deposition time at pH 4.50 (inset: effect of deposition time on peak current). B) DPSC of successive addition of different bismuth concentrations for 200 s to modify the surface of a glassy carbon electrode, from  $E_0$ : 0.00 V to  $E_f$ :  $-1.00$  V C) Current obtained as a function of bismuth concentrations used in the modification by DPSC of the electrode surface. D) Indirect dependence of bismuth concentration on bismuth layer scan rate  $0.100$  V s<sup>-1</sup>.

tentiometry was performed at different bismuth concentrations. For this purpose, we applied a potential of  $-1.00$  V at about 200 s. For a bismuth concentration of  $0$  mmol L<sup>-1</sup> to  $10.00$  mmol L<sup>-1</sup>, the current response can be seen as a time function in Fig. 4B. Here, the bismuth concentration increases while the current decreases. The time range for each concentration is constant, and the current variation is shown as a function of bismuth concentration. We should also mention that electrochemical cleaning was performed between each bismuth addition to ensure that the surface modification was performed under experimental conditions.

In Fig. 4B, we see that the current becomes stable at concentrations ranging from  $0.50$  mmol L<sup>-1</sup> to  $5.00$  mmol L<sup>-1</sup>. However, when the bismuth concentration exceeds  $5.00$  mmol L<sup>-1</sup>, the current does not stabilize and the expected potential step is no longer formed. In the same figure, depicts the concentration of the modifier increases, the current at the electrode surface decreases in small potential steps during the initial modifications at bismuth concentrations from  $0.50$  mmol L<sup>-1</sup> to  $3.00$  mmol L<sup>-1</sup>. When the bismuth concentration reaches  $5.00$  mmol L<sup>-1</sup>, the current decreases in proportion to the increase in concentration. This behavior occurs until the modifier concentration exceeds  $5.00$  mmol L<sup>-1</sup>. To illustrate these observations, Fig. 4C shows the average current of the potential step as a function of bismuth concentration. This shows that the current continues to decrease significantly at concentrations greater than  $5.00$  mmol L<sup>-1</sup>.

The obtained BiE was evaluated indirectly by CV in a bismuth-free solution in buffer at a pH of 4.50 and shows the behavior shown in Fig. 4D. Here, a higher bismuth concentration in the solution leads to a BiE with a higher peak. Even after a concentration of  $2.00$  mmol L<sup>-1</sup>, a linear relationship is seen between the concentration of the modifier solution and the BiE current formed. At concentrations higher than  $7.00$  mmol L<sup>-1</sup>, the peak current of BiE formed drops (not shown) and even detaches some of the material that had accumulated on the surface. Inter-deposit reproducibility also showed that at a bismuth concentration of  $5.00$  mmol L<sup>-1</sup>, the reproducibility between the BiEs

formed was close to 95.0%, using the peak currents obtained for these modifications as a criterion.

### 3.5. Determination of aluminum using BiE

The BiE was used for the determination of aluminum in solution. The best conditions we found for its preparation were: electrodeposition on the surface of the BiE  $5.00$  mmol L<sup>-1</sup> in acetic acid/sodium acetate buffer solution at pH 4.5 by DPSC, application of  $E_0 = 0.00$  V and  $E_f = -1.00$  V against Ag/AgCl for 300 s and completion of electrochemical purification after each measurement.

Existing literature reports that the determination of aluminum in a solution can be improved by the formation of a complex metal ligand in solution<sup>12,14</sup>. One of the most important complexing agents for this determination is cupferron. Experimental parameters that influence the formation of this metal complex include, primarily: the concentration of the complexing agents, the effects of the type of buffer solution used, the pH of the working solutions. We now discuss the optimization of some of these experimental variables, i.e. the effects of the buffer used on the solubility of the complexing agent, the concentration of this agent and its pH for the determination of the cupferron-aluminum metal complex and the spectroscopic characterization of this complex.

#### 3.5.1. Buffer effect on cupferron solubility

To find the best buffer system for the cupferron solutions, two different buffers described in the literature were studied: PIPES and ammonium sulfate buffer<sup>[21,50]</sup>, both with a pH of 5.50. For this purpose, cupferron solutions between  $0.20$  and  $3.00$  mmol L<sup>-1</sup> were prepared in the two buffer systems and Table 1 was prepared for solubility, with the gray color bar indicating that the sample was soluble.

According to Table 1, the best solubility conditions are obtained for cupferron solutions in ammonium sulfate buffer  $0.40$  mmol L<sup>-1</sup>, pH 5.50.

**Table 1**

Dependence of cupferron solubility as a function of concentration of two different buffers (ammonium sulfate and PIPES). The gray bar indicates that the species is soluble.

Buffer	mmol L <sup>-1</sup>	Cupferron/mmol L <sup>-1</sup>			
		1.50	2.00	2.50	3.00
PIPES	0.20				
	0.40				
	0.20				
	0.40				

### 3.5.2. Effect of pH on aluminum solubility

To find the optimum pH for the aluminum solutions in the cupferron/ammonium sulfate system, we studied the aluminum solubility in cupferron solutions 0.22 mmol L<sup>-1</sup> plus ammonium sulfate buffer 0.40 mmol L<sup>-1</sup> in water. The dependence of aluminum concentration on pH is shown in Table 2, where the colored bars indicate the solubility of aluminum in the buffer system at different pH values.

From the results in Table 2, it was found that a pH level of 5.50 is optimum for the preparation of cupferron solutions.

### 3.5.3. Influence of the cupferron concentration on the determination of aluminum with BiE

Ligand concentration is an important factor in the determination of aluminum in a solution. Therefore, different cupferron concentrations from 0.0 mmol L<sup>-1</sup> to 5.00 mmol L<sup>-1</sup> were used in the determination of 0.030 mmol L<sup>-1</sup> aluminum by square wave voltammetry (SWV) with initial and final potentials of 0.00 and -2.00 V, respectively, of BiE in a solution containing ammonium sulfate 0.40 mmol L<sup>-1</sup>, working buffer pH 5.50. The results are shown in Fig. 5.

**Table 2**

Dependence of Al<sup>3+</sup> solubility as a function of pH of a cupferron 0.22 mmol L<sup>-1</sup> solution in ammonium sulfate 0.40 mmol L<sup>-1</sup> buffer. The gray bar indicates that the species is soluble.

pH	Al <sup>3+</sup> /mmol L <sup>-1</sup>			
	3.70 × 10 <sup>-5</sup>	3.70 × 10 <sup>-4</sup>	3.70 × 10 <sup>-3</sup>	3.70 × 10 <sup>-2</sup>
3.50				
4.50				
5.50				
6.50	Formation of precipitates			

Fig. 5A shows that when the concentration of the complexing agent was 0.22 mmol L<sup>-1</sup>, three reduction peaks II<sub>c</sub>, III<sub>c</sub>, and IV<sub>c</sub> were visible at a potential of -1.79, -0.85, and -0.49 V, respectively. When the concentration of the complexing agent is increased to 3.00 mmol L<sup>-1</sup>, the reduction peaks are no longer visible on the graphic scale. According to the results shown in Fig. 5, the most suitable concentration of the complexing agent for the determination of aluminum is 0.22 mmol L<sup>-1</sup>.

### 3.6. Determination of aluminum with BiE

BiE was used to determine aluminum by CV in a solution containing 1.11 × 10<sup>-6</sup> mol L<sup>-1</sup> aluminum in 0.22 mol L<sup>-1</sup> cupferron + ammonium sulfate buffer at pH 5.50. The results of this voltammetry are shown in Fig. 5B. The figure shows the occurrence of the current peak V<sub>a</sub> at a potential of 0.035 V with an I<sub>p</sub> of 135.25 μA. Other aluminum concentrations were also studied and the dependence of the peak current on the aluminum concentration is shown in Fig. 9. The range of concentrations studied was from 1.11 to 4.44 × 10<sup>-6</sup> mol L<sup>-1</sup>. We must keep in mind that the BiE must be formed anew at each voltammetry.

Fig. 5B shows the CVs for three aluminum solutions. In this figure, an increase in I<sub>p</sub> can be seen as the aluminum concentration increases. Fig. 5B shows that as the aluminum concentration increases, I<sub>p</sub> also increases. It should be mentioned that the E<sub>p</sub> in the figure does not represent a linear relationship between I<sub>p</sub> and concentration, in some cases. However, three areas can be defined, two of which show a linear dependence between the concentration and I<sub>p</sub>. In fact, the voltammetric method allowed the quantification of aluminum with detection limits lower than 7.50 ppb, which were calculated experimentally from the minimum aluminum concentration that produced a signal different from the baseline. The lack of linearity in the range studied can be improved. However, techniques such as rectangular voltammetry or differential voltammetry are techniques that allow better detection limits for substances in a solution. For this reason, we decided to determine aluminum with square-wave voltammetry using the bismuth-modified electrodes.

### 3.7. Determination of aluminum using square-wave voltammetry

Fig. 6A shows the square-wave voltammogram of BiE in a solution with and without aluminum. In this figure, two current peaks VI<sub>c</sub> and

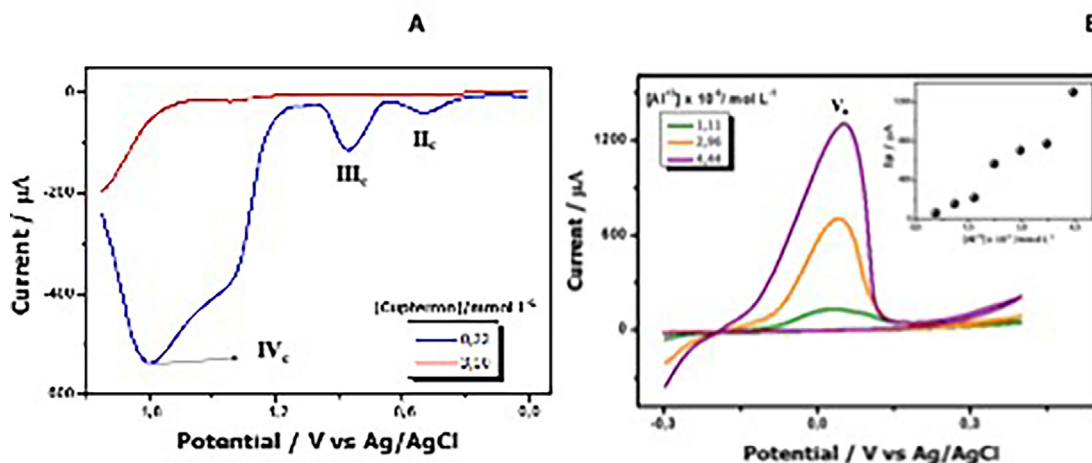


**Fig. 5.** Influence of the concentration of the complexing agent cupferron on the electrochemical determination of aluminum in aqueous solution A) Dependence of cupferron concentration on SWV in ammonium sulphate buffer 0.40 mmol L<sup>-1</sup>, pH 5.50 + 0.030 mmol L<sup>-1</sup> aluminium, with a preconcentration of 30 s at a potential of -2.0 V, frequency: 25 Hz. B) Cyclic voltammetry in cupferron solution 0.22 mmol L<sup>-1</sup> + ammonium sulfate buffer 0.40 mmol L<sup>-1</sup> pH 5.50 from the surface of the glassy carbon electrode modified with bismuth 5.00 mmol L<sup>-1</sup>, scan rate of 0.100 Vs<sup>-1</sup>, φ = 3.00 mm.

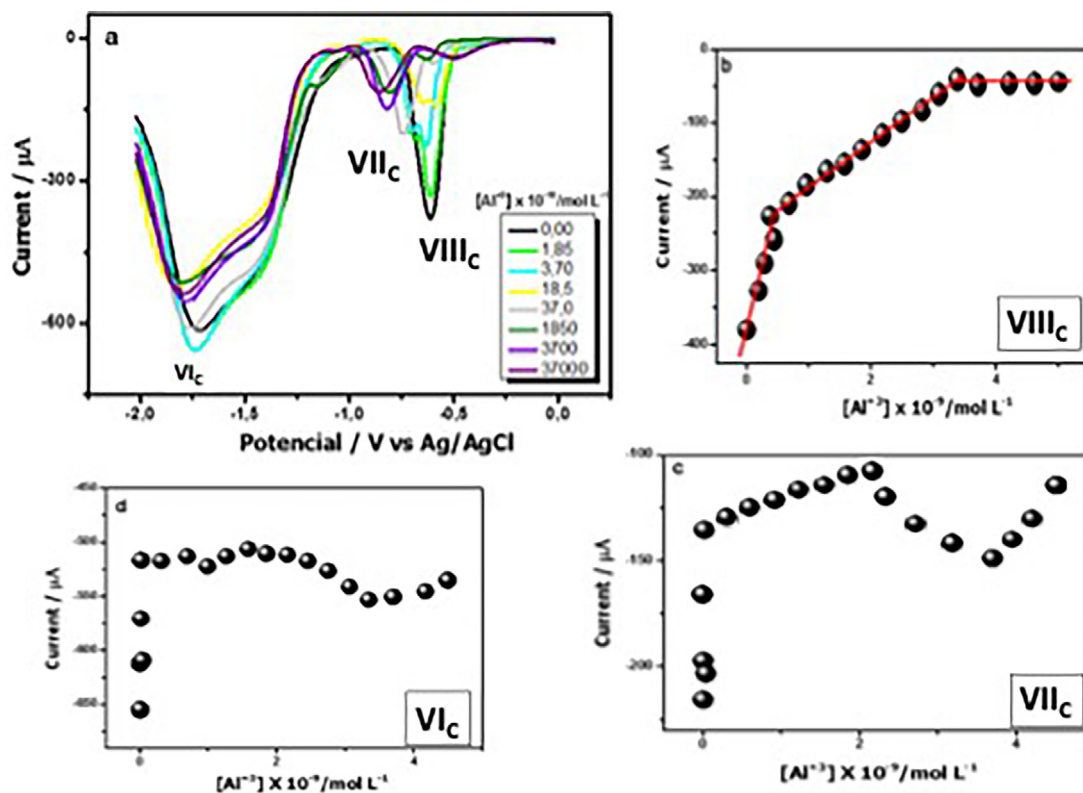


Fig. 6. A) SWV of the electrochemical oxide-reduction of BiE and aluminum in cupferron solution  $0.22 \text{ mmol L}^{-1}$  in ammonium sulfate buffer  $0.4 \text{ mmol L}^{-1}$  pH 5.50, Preconcentration potential:  $-2.50 \text{ V}$ , preconcentration time: 30 s, frequency: 25 Hz,  $\phi = 3 \text{ mm}$  B-D) Indicate the behavior of the  $I_p$  of the indicated peak with respect to the concentration of aluminum.

VIIIc can be seen, the peak VIc at a potential of  $-1.71 \text{ V}$  and with  $I_p$  of  $-614.01 \mu\text{A}$  and a second current peak VIIIc at a potential of  $-0.61 \text{ V}$  and an  $I_p$  of  $-379.19 \mu\text{A}$ . The determination of aluminum in a solution depends on the changes in the peak current VIc-VIIIc. For this reason, the electrochemical behavior was studied by BiE square wave at aluminum concentrations from  $3.70 \times 10^{-10}$  to  $3.70 \times 10^{-5} \text{ mol L}^{-1}$  and the dependence of the peak current on the aluminum concentration (Fig. 6B-D).

Fig. 6A shows the rectangular voltammograms for the determination of aluminum in a solution. The starting point is the BiE with two corresponding current peaks VIc and VIIIc. As the aluminum concentration in the solution increases, these current peaks decrease, and the formation of current peak VIIc can be seen at a potential of  $-0.70 \text{ V}$ . The variation of the three peaks as a function of aluminum concentration is shown in Fig. 6B-D. The current peak VIIIc at a potential of  $-0.60 \text{ V}$  decreases when aluminum is added. The percentage changes in current are smaller than for the other two peaks studied. However, two linear zones can be seen for this peak, which can be used for analytical determination of aluminum in a solution. For the other two peaks (VIc, VIIc), the evaluation of  $I_p$  as a function of aluminum concentration does not show a clear trend. Therefore, the presence of these peaks is not considered.

The linear regions in Fig. 6B, showing  $I_p$ - $I_p$  (initial peak current - final peak current) of BiE as a function of concentration, show how the BiE electrode can be used for the determination of aluminum in a solution. At least 20 separate results confirm that the peak current decreases as a function of aluminum concentration. This data demonstrates the wide range of applications of the BiE for the determination of aluminum in a solution. Fig. 6B shows two apparently linear regions. In the first region we obtain a slope of  $4.00 \times 10^{11} \mu\text{A mol}^{-1}\text{L}$ , while in the second region we

have a slope of  $5.00 \times 10^{10} \mu\text{A mol}^{-1}\text{L}$ . This shows that a linear working range for BiE between concentrations in the range of  $1.85 \times 10^{-10}$  to  $3.70 \times 10^{-6} \text{ mol L}^{-1}$  the sensitivity of the method for the determination of aluminum is large. On the other hand, the detection limit for aluminum using this technique was  $0.025 \text{ ppb}$ , which is 300 times lower than the values determined by cyclic voltammetry.

We have attempted to establish a relationship between the sensitivity of the electrode to the determination of  $\text{Al}^{3+}$  and the size of the bismuth particles carried on the surface of the carbon electrode, as analyzed by SEM images (Fig. S1) and the size of the bismuth particles carried on the surface of the carbon electrode, as analyzed by SEM images. However, it was not possible to establish a definite relationship in this dependence. To demonstrate this relationship, the determination of  $\text{Al}^{3+} 1.85 \times 10^{-10} \text{ mol L}^{-1}$  was carried out under the conditions shown in Fig. 6 for different concentrations of bismuth in the preparation of BiE, where the peak current at a potential of  $-0.62 \text{ V}$  was performed under the conditions shown in Fig. 6 for different concentrations of bismuth in the preparation of BiE, evaluating the peak current at a potential of  $-0.62 \text{ V}$  (Fig. S2). In this way, we confirm that the concentration of bismuth  $5.00 \text{ mmol L}$ , allowed us to obtain the greatest sensitivity in the determination of aluminum.

In order to find the best possible selectivity of the BiE for the detection of  $\text{Al}^{3+}$ , a solution containing  $1.00 \times 10^{-9} \text{ mol L}^{-1}$  of  $\text{Pb}^{2+}$ ,  $\text{Cd}^{2+}$  and  $\text{Zn}^{2+}$ , was studied under the same conditions as in Fig. 6. It was found that the reduction potentials for these ions in solution are  $-0.50$ ,  $-0.72$  y  $-1.08 \text{ V}$  respectively (Fig. S3), which is different from the reduction potential of  $\text{Al}^{3+}$  ( $-0.61 \text{ V}$ ) under the same conditions, indicating that these metals do not interfere with the determination of aluminum in solution.

#### 4. Conclusions

The surface of a glassy carbon electrode was modified by the electrochemical reduction of bismuth in a 1.00 mol L<sup>-1</sup> acetate buffer at a pH of 4.50. The modification was evaluated by cyclic voltammetry, examining the effects of some experimental variables. Our results show that the final potential in a double-potential pulse chronoamperometry must be -1.00 V, using a deposition time of 300 s in a 5.00-mmol L<sup>-1</sup> bismuth solution and performing an electrochemical cleanup between each measurement. This method ensures reproducible and stable surface modification, which is used to determine aluminum in a solution containing cupferron plus (NH<sub>4</sub>)<sub>2</sub>SO<sub>4</sub> at a pH of 5.50. Cupferron and aluminum thereby form a complex that could be characterized by IR and UV-VIS spectroscopy. This complex produces a sensitive current peak at -0.60 V vs. Ag/AgCl when determined by square wave voltammetry in the concentration range of 1.85 × 10<sup>-10</sup> to 3.70 × 10<sup>-6</sup> mol L<sup>-1</sup> with a detection limit of 0.025 ppb.

#### CRediT authorship contribution statement

**Maria Camila Ayala:** Conceptualization, Methodology, Validation, Visualization, Writing – original draft, Writing – review & editing. **Lizbeth Lorena López:** Formal analysis, Investigation, Methodology, Validation, Visualization, Writing – review & editing. **Andres Jaramillo-Botero:** Conceptualization, Investigation, Methodology, Validation, Visualization, Writing – review & editing. **Drochss Valencia:** Conceptualization, Formal analysis, Investigation, Methodology, Software, Validation, Writing – original draft, Writing – review & editing.

#### Declaration of Competing Interest

The authors declare that they have no known competing financial interests or personal relationships that could have appeared to influence the work reported in this paper.

#### Acknowledgments

This work was partially funded by the “OMICAS program: Optimización Multiescala In-silico de Cultivos Agrícolas Sostenibles (Infraestructura y validación en Arroz y Caña de Azúcar)” Scientific Ecosystem belonging to the Colombia Científica Program, sponsored by The World Bank, The Ministry of Science, Technology and Innovation (MINCIENCIAS), ICETEX, the Colombian Ministry of Education and the Colombian Ministry of Commerce, Industry and Tourism, under GRANT ID: FP44842-217-2018, OMICAS Award ID: 792-61187.

#### Appendix A. Supplementary data

Supplementary data to this article can be found online at <https://doi.org/10.1016/j.jelechem.2022.116552>.

#### References

- [1] F. Valentini, M. Carbone, G. Palleschi, *Anal. Bioanal. Chem.* **405** (2013) 451.
- [2] H. El-Mai, E. Espada-Bellido, M. Stitou, M. García-Vargas, M.D. Galindo-Riaño, *Talanta* **151** (2016) 14.
- [3] A.K. Srivastava, S.S. Upadhyay, C.R. Rawool, N.S. Punde, A.S. Rajpurohit, *Curr. Anal. Chem.* **15** (2019) 249.
- [4] W. Ye, Y. Li, J. Wang, B. Li, Y. Cui, Y. Yang, G. Qian, *J. Solid State Chem.* **281** (2020) 121032.
- [5] F. Wolfart, B.M. Hryniewicz, M.S. Goes, C.M. Correa, R. Torresi, M.A.O.S. Minadeo, S.I.C. de Torresi, R.D. Oliveira, L.F. Marchesi, M. Vidotti, *J. Solid State Chem.* **21** (2017) 2489.
- [6] N. Baig, M. Sajid, T.A. Saleh, *Trends Anal. Chem.* **111** (2019) 47.
- [7] Z. Wang, E. Liu, X. Zhao, *Thin Solid Films* **519** (2011) 5285.
- [8] A. Economou, *TrAC Trends in Anal. Chem.* **24** (2005) 334.
- [9] M. Baghayeri, H. Alinezhad, M. Fayazi, M. Tarahomi, R. Ghanei-Motlagh, B. Maleki, *Electrochim Acta* **312** (2019) 80.
- [10] M.A. Deshmukh, H.K. Patil, G.A. Bodkhe, M. Yasuzawa, P. Koinkar, A. Ramanaviciene, M.D. Shirsat, A. Ramanavicius, *Sens. Actuator B-Chem.* **260** (2018) 331.
- [11] V.B. dos Santos, E.L. Fava, N.S. de Miranda Curi, R.C. Faria, O. Fatibello-Filho, *Talanta* **126** (2014) 82.
- [12] O. Domínguez-Renedo, A. Marta Navarro-Cuñado, E. Ventas-Romay, M. Asunción Alonso-Lomillo, *Talanta* **196** (2019) 131.
- [13] A.J. Downard, H. Kipton, J. Powell, S. Xu, *Anal. Chim. Acta* **251** (1991) 157.
- [14] S.K. Mittal, M. Chhibber, S. Gupta, *Microchem. J.* **168** (2021) 106500.
- [15] A. Ahmadi, A. Nezamzadeh-Ejhi, *J. Electroanal. Chem.* **801** (2017) 328.
- [16] C.Y. Yao, W.L. Fu, *World J. Gastroenterol.* **20** (2014) 12485.
- [17] K.A. Mahmoud, J.H.T. Luong, *Anal. Lett.* **43** (2010) 1680.
- [18] Z. Amani-Beni, A.J. Nezamzadeh-Ejhi, *Colloid. Interface. Sci.* **504** (2017) 186.
- [19] S. Mahalingam, A. Manap, A. Omar, F.W. Low, N.F. Afandi, C.H. Chia, N.A. Rahim, *Renew. Sust. Energ. Rev.* (2021) 144.
- [20] S. Kim, O. Dovjuu, S.H. Choi, H. Jeong, J.T. Park, *Coatings* (2019) 9.
- [21] G. Kefala, A. Economou, M. Sofoniu, *Talanta* **68** (2006) 1013.
- [22] S.T. Palisoc, R.V.M. Chua, M.T. Natividad, *Materials Research Express* **7** (2020) 015081.
- [23] Á. Vilas-Boas, P. Valderrama, N. Fontes, D. Geraldo, F. Bento, *Food Chem.* **276** (2019) 719.
- [24] J.G. Osteryoung, R.A. Osteryoung, *Anal. Chem.* **57** (1985) 101.
- [25] Y. Wu, P. Deng, Y. Tian, Z. Ding, G. Li, J. Liu, Z. Zuberi, Q. He, *Bioelectrochemistry* **131** (2020) 107393.
- [26] V.K. Sharma, F. Jelen, L. Trnkova, *Sensors-Basel* **15** (2015) 1564.
- [27] A. Niknezhadi, A. Nezamzadeh-Ejhi, *J. Colloid Interface Sci.* **501** (2017) 321.
- [28] Nezamzadeh-Ejhi, A.; Shahanshahi, M. *J. Ind. Eng. Chem.* **2013**, *19*, 2026.
- [29] T. Tamiji, A. Nezamzadeh-Ejhi, *J. Electroanal. Chem.* **829** (2018) 95.
- [30] P. Nayak, N. Kurra, C. Xia, H.N. Alshareef, *Adv. Electron. Mater.* **2** (2016) 1600185.
- [31] S.A. Perdomo, V. Ortega, A. Jaramillo-Botero, N. Mancilla, J.H. Mosquera-DeLaCruz, D.P. Valencia, M. Quimbaya, J.D. Contreras, G.E. Velez, O.A. Loaliza, A. Gómez, J.d.l. Roche, *IEEE Trans. Instrum. Meas.* **70** (2021) 1.
- [32] D.P. Valencia, L.M.F. Dantas, A. Lara, J. Garcia, Z. Rivera, J. Rosas, M. Bertotti, *J. Electroanal. Chem.* **770** (2016) 50.
- [33] M. Nosuhi, A. Nezamzadeh-Ejhi, *J. Electroanal. Chem.* **810** (2018) 119.
- [34] E. Coy, L. Yate, D.P. Valencia, W. Aperador, K. Siuzdak, P. Torruella, E. Azanza, S. Estrade, I. Iatsunskiy, F. Peiro, X. Zhang, J. Tejada, R.F. Ziolo, *ACS Appl. Mater. Interfaces* **9** (2017) 30872.
- [35] D.P. Valencia, L. Yate, W. Aperador, Y. Li, E. Coy, *J. Phys. Chem. C* **122** (2018) 25433.
- [36] A.T. Jan, M. Azam, K. Siddiqui, A. Ali, I. Choi, Q.M.R. Haq, *Int. J. Mol. Sci.* **16** (2015) 29592.
- [37] J. Briffa, E. Sinagra, R. Blundell, *Heliyon* **6** (2020) e04691.
- [38] J. Barceló, C. Poschenrieder, *J. Plant Nutr.* **13** (1990) 1.
- [39] S.K. Jaiswal, J. Naamala, F.D. Dakora, *Biol. Fertil. Soils* **54** (2018) 309.
- [40] O. Drabek, L. Boruvka, L. Mladkova, M. Kocarek, *J. Inorg. Biochem.* **97** (2003) 8.
- [41] Y. Xie, Z. Guan, J. Cheng, Y. Zhou, M. Yan, *Chemosphere* **270** (2021) 128655.
- [42] C. de Aragão Tannus, F. de Souza Dias, F.B. Santana, D.C.M.B. dos Santos, H.I.F. Magalhães, F. de Souza Dias, de Freitas Santos Júnior, A. *Biol. Trace Elem. Res.* **199** (2021) 2330.
- [43] H. Park, W. Kim, M. Kim, G. Lee, W. Lee, J. Park, *Spectrochim. Acta A Mol. Biomol. Spectrosc.* **245** (2021) 118880.
- [44] N. Raeisi-Kheirabadi, A. Nezamzadeh-Ejhi, H. Aghaei, *Iran. J. Catal.* **11** (2021) 181.
- [45] A.L. Eckermann, D.J. Feld, J.A. Shaw, T.J. Meade, *Coord. Chem. Rev.* **254** (2010) 1769.
- [46] A.E. Thorarinsdottir, C. Costentin, S.S. Veroneau, D.G. Nocera, *Chem. Mater.* **34** (2022) 826.
- [47] Z. Gong, M. Zhang, G. Yao, J. Lv, X. Jiang, L. Yang, Y. Cheng, J. Tao, X. Wang, Z. Wang, G. He, Z. Sun, *J. Electrochem. Soc.* **163** (2016) E328.
- [48] S. Demiri, M. Najdoski, J. Velevska, *Mater. Res. Bull.* **46** (2011) 2484.
- [49] E.V. Zolotukhina, I.S. Bezverkhy, M.A. Vorotyntsev, *Electrochim. Acta* **122** (2014) 247.
- [50] J. Wasag, M. Grabarczyk, *Talanta* **233** (2021) 122565.